

# Supplementary Materials: Spatial-Temporal Knowledge Transfer for Dynamic Constrained Multiobjective Optimization

Zhenzhong Wang, Dejun Xu, Min Jiang, *Senior Member, IEEE*, and Kay Chen Tan, *Fellow, IEEE*

**Abstract**—This supplementary material includes two tables and sixteen figures. Table S-I reports the MHV values obtained by different algorithms. To validate the effectiveness of the designed TKT, the MIGD and MHV values of DC-MFEA and DC-MFEA<sub>w/o-TKT</sub> are recorded in Table S-II. To investigate the influence of the parameter  $N_{T2}$ , convergence traces of average IGD and average HV values obtained are plotted in Fig. S-1 and Fig. S-2, respectively. Fig. S-3 ~ Fig. S-16 show the visualization of DCPOF, DUPOF, and feasible areas of DCF1 ~ DCF14, respectively.

DCF1:

$$\begin{aligned} \min & \left\{ \begin{array}{l} f_1(x) = x_1 \\ f_2(x) = g\sqrt{1-f_1^2} \end{array} \right. \\ \text{s.t. } & c(x) = l_1 + 0.5 \sin(t+l_2)^{10} \leq 0 \\ & G(t) = 0.5|\sin(0.5\pi t)| \\ & g = 1 + 0.1(|\sum_{i=2}^D x_i - G|)^{0.5} \\ & l_1 = 1 - f_1^2 - f_2^2 \\ & l_2 = 5\sqrt{2}\pi f_2 - \sqrt{2}f_1 - 1 \end{aligned} \quad (1)$$

DCF1 has a changing feasible region. The DCPOF and DUPOF are totally overlapped, and the feasible region is connected by DCPOF. Although the connectivity of the feasible region is connected, narrow connectivity challenges the algorithm. DCF1 is plotted in Fig. S-3. The search space is  $[0, 1]^D$ .

DCF2:

This work was supported in part by the National Natural Science Foundation of China under Grant U21A20512; in part by the National Natural Science Foundation of China under Grant 62276222; in part by the Research Grants Council of the Hong Kong under Grant PolyU11211521 and Grant PolyU15218622; in part by the Hong Kong Polytechnic University (Project No.: 1-ZEOC). (*Corresponding authors: Min Jiang*).

Zhenzhong Wang and Kay Chen Tan are with the Department of Computing, The Hong Kong Polytechnic University, Hong Kong SAR, China (e-mail: zhenzhong16.wang@connect.polyu.hk; kctan@polyu.edu.hk).

Min Jiang and Dejun Xu are with the Department of Artificial Intelligence, Key Laboratory of Digital Protection and Intelligent Processing of Intangible Cultural Heritage of Fujian and Taiwan, Ministry of Culture and Tourism, School of Informatics, Xiamen University, Xiamen 361005, Fujian, China (e-mail: minjiang@xmu.edu.cn).

$$\begin{aligned} \min & \left\{ \begin{array}{l} f_1(x) = x_1 \\ f_2(x) = g(0.5 + G - f_1) \end{array} \right. \\ \text{s.t. } & c(x) = l_1 + 0.6 \sin(2t + l_2)^4 \leq 0 \\ & G(t) = 0.5|\sin(t)| \\ & g = 1 + 0.1(|\sum_{i=2}^D x_i - G|)^{0.5} \\ & l_1 = 0.55 + G - f_1 - f_2 \\ & l_2 = 2\sqrt{2}\pi f_2 - \sqrt{2}f_1 - 1 \end{aligned} \quad (2)$$

DCF2 also has a changing feasible region, and the changing DCPOF and DUPOF of DCF2 are overlapped. In addition, DCF2 has a changing search space  $[0, 0.5 + G]^D$ . DCF2 is plotted in Fig. S-4.

DCF3:

$$\begin{aligned} \min & \left\{ \begin{array}{l} f_1(x) = x_1 \\ f_2(x) = g\sqrt{1-f_1^2} \end{array} \right. \\ \text{s.t. } & \left\{ \begin{array}{l} c_1(x) = 1.1 + C - f_1^2 - f_2^2 \leq 0 \\ c_2(x) = (1 + 0.5 \sin(6l))^2 - f_1^2 - f_2^2 \leq 0 \end{array} \right. \\ & G(t) = |\sin(t)| \\ & g = 1 + 0.1(|\sum_{i=2}^D x_i - G|)^{0.5} \\ & C(t) = |\sin(t)| \\ & l = 0.5\pi - 2|\arctan \frac{f_2}{f_1} - 0.25\pi| \end{aligned} \quad (3)$$

The DCPOF of DCF3 is a part of the DUPOF. DCF3 has multiple constraints, and the constraints make the changing feasible region disconnected. The search space is  $[0, 1]^D$ . DCF3 is plotted in Fig. S-5.

DCF4:

$$\begin{aligned} \min & \left\{ \begin{array}{l} f_1(x) = x_1 \\ f_2(x) = g\sqrt{1-f_1^2} \end{array} \right. \\ \text{s.t. } & \left\{ \begin{array}{l} c_1(x) = 1.1 + C - f_1^2 - f_2^2 \leq 0 \\ c_2(x) = (1 + 0.6 \sin(t + 6l))^2 - f_1^2 - f_2^2 \leq 0 \end{array} \right. \\ & G(t) = |\sin(t)| \\ & g = 1 + 0.1(|\sum_{i=2}^D x_i - G|)^{0.5} \\ & C(t) = |\sin(t)| \\ & l = 0.5\pi - 2|\arctan \frac{f_2}{f_1} - 0.25\pi| \end{aligned} \quad (4)$$

The changing DCPOF of DCF4 is always a part of the unchanged DUPOF. The multiple constraints make the changing feasible region disconnected. At the same time, the number of disconnected feasible regions changes over time. The search space is  $[0, 1]^D$ . DCF4 is plotted in Fig. S-6.

TABLE S-I  
MEAN AND STANDARD DEVIATION VALUES OF MHV METRIC OBTAINED BY COMPETING ALGORITHMS FOR DIFFERENT DYNAMIC TEST FUNCTIONS UNDER VARIOUS TEST SETTINGS

Problem	$n_t, \tau_t$	DC-MFEA	DNSGAI-CDP	DC-MOEA	KT-NSGAI-CDP	dCMOEA	CTAEA
DCF1	1,20	<b>3.97e-01(7.60e-06)</b>	2.56e-01(1.63e-04)+	2.75e-01(2.76e-06)+	2.69e-01(1.68e-05)+	1.56e-01(1.36e-04)+	3.17e-01(5.54e-07)+
	10,20	<b>3.75e-01(1.82e-06)</b>	2.99e-01(3.46e-04)+	3.12e-01(2.62e-06)+	2.61e-01(2.10e-05)+	1.72e-01(2.48e-04)+	3.56e-01(9.79e-07)+
	10,10	<b>3.54e-01(8.45e-06)</b>	2.93e-01(2.06e-04)+	3.07e-01(9.49e-07)+	2.61e-01(1.34e-05)+	2.31e-01(1.18e-04)+	3.34e-01(2.50e-06)+
DCF2	1,20	6.28e-01(2.49e-08)	6.14e-01(5.40e-05)+	6.08e-01(1.20e-06)+	6.02e-01(2.51e-06)+	3.84e-01(3.02e-04)+	<b>6.31e-01(1.49e-08)-</b>
	10,20	6.35e-01(1.60e-08)	6.20e-01(5.47e-05)+	6.13e-01(3.05e-07)+	6.08e-01(4.71e-07)+	3.81e-01(1.40e-06)+	<b>6.36e-01(3.64e-08)-</b>
	10,10	<b>6.33e-01(3.9e-08)</b>	6.19e-01(3.42e-05)+	6.03e-01(1.29e-06)+	6.09e-01(2.19e-06)+	4.00e-01(2.30e-05)+	6.32e-01(6.61e-07)+
DCF3	1,20	<b>4.80e-01(9.63e-07)</b>	4.21e-01(1.83e-04)+	4.39e-01(2.46e-06)+	3.99e-01(9.06e-06)+	2.77e-01(5.90e-05)+	4.77e-01(8.98e-07)+
	10,20	<b>4.97e-01(5.24e-07)</b>	4.20e-01(1.59e-04)+	4.40e-01(1.48e-06)+	3.99e-01(5.21e-06)+	2.81e-01(4.73e-04)+	4.80e-01(9.05e-07)+
	10,10	<b>4.87e-01(3.31e-07)</b>	4.18e-01(9.90e-05)+	4.30e-01(1.68e-06)+	4.01e-01(1.74e-06)+	3.03e-01(8.66e-05)+	4.57e-01(1.09e-06)+
DCF4	1,20	<b>4.20e-01(4.32e-07)</b>	3.35e-01(4.93e-04)+	3.59e-01(2.53e-05)+	3.41e-01(3.47e-06)+	2.13e-01(2.41e-04)+	4.13e-01(1.28e-06)+
	10,20	<b>4.34e-01(2.23e-07)</b>	3.31e-01(7.10e-04)+	3.54e-01(4.57e-05)+	3.39e-01(2.06e-06)+	1.98e-01(5.82e-04)+	4.13e-01(1.51e-06)+
	10,10	<b>4.24e-01(1.62e-07)</b>	3.29e-01(7.61e-04)+	3.58e-01(3.43e-06)+	3.38e-01(3.96e-06)+	2.17e-01(1.15e-03)+	3.92e-01(3.49e-06)+
DCF5	1,20	<b>3.39e-01(2.62e-08)</b>	3.04e-01(4.57e-05)+	2.90e-01(8.69e-06)+	2.99e-01(1.23e-06)+	1.47e-01(1.06e-04)+	3.39e-01(1.14e-07)=
	10,20	<b>3.45e-01(5.75e-08)</b>	3.08e-01(7.28e-05)+	2.93e-01(7.33e-05)+	3.02e-01(5.06e-06)+	1.49e-01(7.15e-05)+	3.44e-01(4.77e-07)+
	10,10	<b>3.43e-01(2.44e-07)</b>	3.06e-01(5.13e-05)+	2.81e-01(1.36e-05)+	3.04e-01(4.09e-06)+	1.69e-01(1.33e-05)+	3.39e-01(3.43e-07)+
DCF6	1,20	<b>1.30e-01(3.29e-07)</b>	1.16e-01(9.42e-06)+	1.21e-01(2.17e-07)+	1.14e-01(3.40e-07)+	4.82e-02(1.23e-04)+	1.17e-01(5.37e-07)+
	10,20	<b>1.32e-01(5.78e-09)</b>	1.15e-01(9.20e-06)+	1.20e-01(5.70e-08)+	1.14e-01(1.30e-07)+	5.53e-02(1.83e-04)+	1.17e-01(1.02e-06)+
	10,10	<b>1.31e-01(4.15e-08)</b>	1.15e-01(4.49e-06)+	1.18e-01(9.57e-08)+	1.14e-01(2.63e-07)+	8.65e-02(3.91e-05)+	1.13e-01(9.64e-07)+
DCF7	1,20	<b>3.40e-01(1.17e-05)</b>	2.88e-01(2.53e-04)+	3.05e-01(1.00e-06)+	2.60e-01(1.26e-05)+	2.30e-01(6.40e-05)+	2.97e-01(4.78e-06)+
	10,20	<b>3.62e-01(6.91e-07)</b>	2.87e-01(2.03e-04)+	3.06e-01(5.09e-06)+	2.62e-01(1.60e-05)+	2.33e-01(1.01e-04)+	3.01e-01(9.51e-06)+
	10,10	<b>3.54e-01(2.66e-06)</b>	2.85e-01(1.17e-04)+	2.99e-01(7.49e-06)+	2.61e-01(3.21e-06)+	2.40e-01(8.85e-06)+	2.71e-01(3.00e-05)+
DCF8	1,20	<b>6.56e-01(2.67e-06)</b>	6.32e-01(3.57e-05)+	6.38e-01(1.91e-05)+	6.16e-01(1.35e-05)+	5.55e-01(5.23e-05)+	6.41e-01(1.20e-05)+
	10,20	<b>6.49e-01(1.76e-06)</b>	6.19e-01(6.01e-05)+	6.30e-01(3.17e-06)+	6.04e-01(1.35e-05)+	5.42e-01(1.57e-04)+	6.32e-01(1.06e-05)+
	10,10	<b>6.47e-01(3.42e-06)</b>	6.17e-01(4.65e-05)+	6.23e-01(3.13e-05)+	6.01e-01(9.81e-06)+	5.63e-01(2.24e-05)+	6.13e-01(1.13e-05)+
DCF9	1,20	<b>3.69e-01(4.41e-07)</b>	3.51e-01(5.13e-05)+	3.35e-01(1.62e-05)+	3.28e-01(1.58e-05)+	3.28e-01(8.26e-06)+	3.41e-01(6.32e-06)+
	10,20	<b>3.82e-01(3.79e-07)</b>	3.65e-01(4.82e-05)+	3.44e-01(1.64e-05)+	3.39e-01(1.47e-05)+	1.95e-01(1.29e-05)+	3.55e-01(5.64e-06)+
	10,10	<b>3.82e-01(4.93e-07)</b>	3.61e-01(7.18e-05)+	3.28e-01(2.28e-05)+	3.37e-01(1.88e-05)+	1.92e-01(4.97e-05)+	3.39e-01(5.80e-06)+
DCF10	1,20	1.49e+00(1.25e-02)	1.43e+00(7.62e-02)=	<b>1.68e+00(1.03e-02)</b>	6.81e-01(4.59e-03)+	1.16e+00(1.55e-03)+	1.42e+00(3.13e-03)=
	10,20	1.48e+00(3.67e-03)	1.37e+00(5.66e-02)	<b>1.57e+00(8.51e-03)</b>	6.81e-01(3.29e-03)+	1.23e+00(4.52e-04)+	1.41e+00(1.47e-02)=
	10,10	1.50e+00(1.27e-02)	1.30e+00(1.24e-02)	<b>1.57e+00(3.57e-03)</b>	5.87e-01(4.58e-03)+	1.21e+00(1.99e-03)+	1.26e+00(5.51e-03)+
DCF11	1,20	8.56e-01(5.60e-04)	7.11e-01(1.85e-02)=	5.26e-01(2.17e-04)=	7.91e-01(1.98e-03)=	4.74e-01(1.20e-02)+	<b>1.06e+00(4.52e-04)</b>
	10,20	9.82e-01(1.85e-03)	7.33e-01(2.68e-02)	5.35e-01(4.82e-04)=	7.53e-01(1.92e-03)=	5.44e-01(1.38e-02)+	<b>1.05e+00(4.28e-04)</b>
	10,10	8.42e-01(1.62e-03)	7.08e-01(1.56e-02)	5.38e-01(4.59e-04)=	7.77e-01(1.25e-03)=	6.39e-01(1.24e-03)=	<b>1.00e+00(2.72e-03)</b>
DCF12	1,20	2.32e-01(1.22e-03)	6.91e-01(8.28e-02)	4.28e-01(7.38e-04)=	4.30e-01(8.53e-04)=	4.62e-01(4.33e-03)=	<b>1.30e+00(1.46e-03)</b>
	10,20	5.03e-01(4.75e-03)	6.69e-01(7.05e-02)	4.25e-01(1.99e-04)=	4.28e-01(2.11e-03)=	5.49e-01(1.47e-02)=	<b>1.21e+00(2.51e-03)</b>
	10,10	4.92e-01(8.89e-03)	6.87e-01(8.21e-02)	4.39e-01(9.51e-05)=	4.60e-01(1.07e-03)=	8.61e-01(2.36e-03)=	<b>1.07e+00(4.02e-03)</b>
DCF13	1,20	6.07e-01(5.28e-04)	6.48e-01(1.22e-03)	6.76e-01(2.84e-04)=	6.21e-01(9.32e-04)=	6.01e-01(1.19e-03)=	<b>7.29e-01(3.61e-03)</b>
	10,20	5.67e-01(1.59e-03)	6.21e-01(1.01e-03)	6.41e-01(1.12e-03)=	6.18e-01(4.02e-04)=	5.46e-01(2.18e-03)=	<b>7.44e-01(1.58e-03)</b>
	10,10	5.46e-01(3.65e-04)	6.37e-01(1.03e-03)	<b>6.64e-01(1.55e-04)</b>	5.94e-01(2.76e-04)=	5.81e-01(2.01e-03)=	6.46e-01(1.02e-03)
DCF14	1,20	<b>1.17e+00(1.68e-04)</b>	7.31e-01(5.58e-02)+	1.13e+00(8.03e-04)=	9.15e-01(1.07e-03)+	6.14e-01(1.97e-02)+	1.10e+00(5.20e-04)+
	10,20	<b>1.16e+00(1.73e-04)</b>	7.84e-01(1.56e-02)+	1.12e+00(4.68e-04)=	1.07e+00(4.90e-04)+	8.02e-01(2.90e-03)+	1.05e+00(1.63e-03)+
	10,10	<b>1.14e+00(3.36e-04)</b>	7.93e-01(1.33e-02)+	1.13e+00(2.10e-04)=	1.05e+00(1.08e-03)+	8.78e-01(3.87e-03)+	9.58e-01(3.25e-03)+

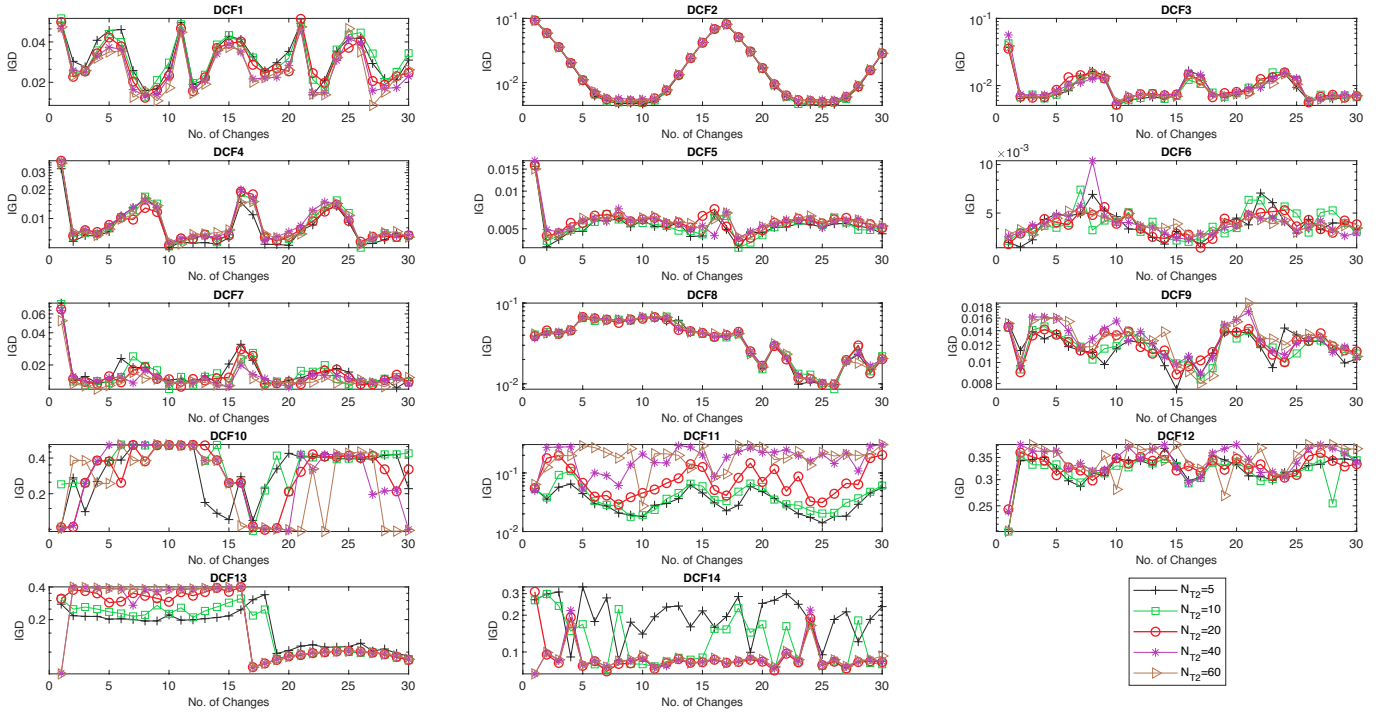


Fig. S-1. Convergence traces of average IGD values obtained by DC-MFEA with different values of  $N_{T2}$ .

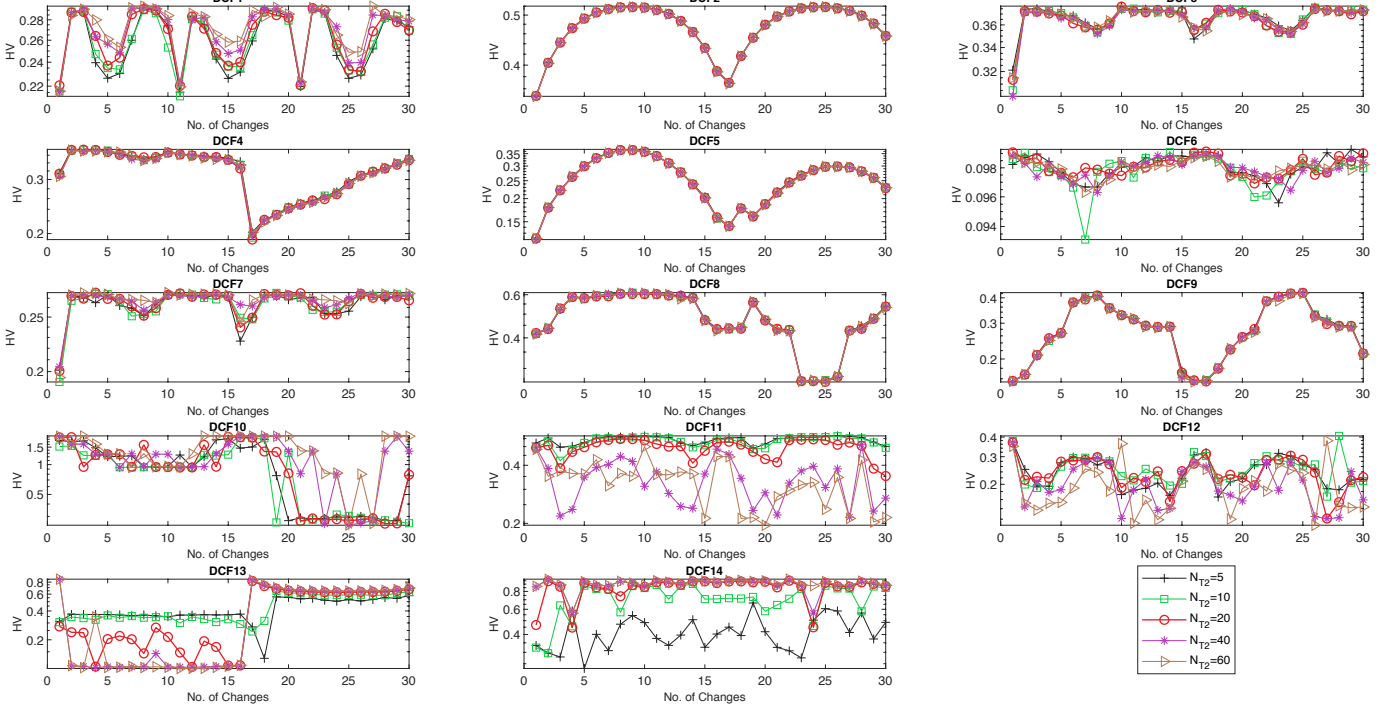


Fig. S-2. Convergence traces of average HV values obtained by DC-MFEA with different values of  $N_{T2}$ .

TABLE S-II  
MEAN AND STANDARD DEVIATION VALUES OF MIGD AND MHV METRICS OBTAINED BY DC-MFEA AND DC-MFEA<sub>w/o-TKT</sub> UNDER VARIOUS TEST SETTINGS

Problem	$n_t, \tau_t$	MIGD		MHV	
		DC-MFEA	DC-MFEA <sub>w/o-TKT</sub>	DC-MFEA	DC-MFEA <sub>w/o-TKT</sub>
DCF1	1,20	<b>2.57e-02(4.58e-06)</b>	9.18e-02(2.97e-06)+	<b>3.97e-01(7.60e-06)</b>	3.08e-01(2.07e-06)+
	10,20	<b>4.41e-02(5.53e-07)</b>	5.42e-02(1.17e-06)+	<b>3.75e-01(1.82e-06)</b>	3.60e-01(7.78e-07)+
	10,10	<b>6.07e-02(3.30e-06)</b>	6.89e-02(7.11e-07)+	<b>3.54e-01(8.45e-06)</b>	3.43e-01(6.67e-08)+
DCF2	1,20	4.96e-02(7.05e-09)	<b>4.95e-02(3.76e-09)=</b>	6.28e-01(2.49e-08)	<b>6.29e-01(1.42e-08)=</b>
	10,20	<b>4.45e-02(5.38e-09)</b>	4.47e-02(1.91e-09)+	<b>6.35e-01(1.60e-08)</b>	6.35e-01(4.84e-09)+
	10,10	<b>4.54e-02(4.18e-09)</b>	4.59e-02(1.27e-08)+	<b>6.33e-01(1.39e-08)</b>	6.32e-01(3.44e-08)+
DCF3	1,20	2.55e-02(8.16e-07)	<b>2.40e-02(2.30e-07)=</b>	4.80e-01(9.63e-07)	<b>4.82e-01(1.19e-06)=</b>
	10,20	<b>1.38e-02(2.20e-07)</b>	2.21e-02(6.46e-08)+	<b>4.97e-01(5.24e-07)</b>	4.85e-01(4.81e-07)+
	10,10	<b>2.08e-02(1.36e-07)</b>	3.43e-02(5.50e-07)+	<b>4.87e-01(3.31e-07)</b>	4.67e-01(2.24e-06)+
DCF4	1,20	<b>2.40e-02(2.07e-07)</b>	2.35e-02(1.19e-07)=	4.20e-01(4.32e-07)	<b>4.22e-01(5.99e-07)=</b>
	10,20	<b>1.31e-02(1.80e-08)</b>	2.07e-02(2.39e-06)+	<b>4.34e-01(2.23e-07)</b>	4.23e-01(3.96e-06)+
	10,10	<b>1.98e-02(2.08e-07)</b>	3.40e-02(6.58e-07)+	<b>4.24e-01(1.62e-07)</b>	4.04e-01(1.17e-06)+
DCF5	1,20	1.12e-02(1.21e-08)	<b>1.07e-02(4.19e-08)=</b>	3.39e-01(2.62e-08)	<b>3.40e-01(3.01e-08)=</b>
	10,20	<b>9.72e-03(1.93e-08)</b>	1.05e-02(1.45e-08)+	<b>3.45e-01(5.75e-08)</b>	3.44e-01(9.31e-08)+
	10,10	<b>1.17e-02(6.50e-08)</b>	1.31e-02(1.24e-07)+	<b>3.43e-01(2.44e-07)</b>	3.42e-01(2.17e-07)+
DCF6	1,20	<b>1.06e-02(2.11e-06)</b>	1.31e-02(5.99e-07)=	<b>1.30e-01(3.29e-07)</b>	1.29e-01(1.25e-07)=
	10,20	<b>6.67e-03(6.68e-09)</b>	1.39e-02(2.37e-06)+	<b>1.32e-01(5.78e-09)</b>	1.28e-01(3.49e-07)+
	10,10	<b>8.19e-03(7.71e-07)</b>	2.35e-02(5.15e-07)+	<b>1.31e-01(4.15e-08)</b>	1.24e-01(3.74e-08)+
DCF7	1,20	<b>4.58e-02(1.62e-05)</b>	4.20e-02(1.45e-05)=	3.40e-01(1.17e-05)	<b>3.43e-01(1.02e-05)=</b>
	10,20	<b>2.92e-02(6.65e-07)</b>	4.27e-02(1.87e-05)+	<b>3.62e-01(6.91e-07)</b>	3.43e-01(9.31e-06)+
	10,10	<b>3.41e-02(2.43e-06)</b>	6.30e-02(7.74e-06)+	<b>3.54e-01(2.66e-06)</b>	3.24e-01(2.63e-06)+
DCF8	1,20	<b>7.72e-02(2.19e-06)</b>	7.89e-02(8.61e-07)=	<b>6.56e-01(2.67e-06)</b>	6.55e-01(6.25e-07)=
	10,20	8.01e-02(9.36e-07)	<b>7.79e-02(5.57e-06)=</b>	<b>6.49e-01(1.76e-06)</b>	6.46e-01(4.15e-06)=
	10,10	<b>7.78e-02(1.13e-06)</b>	7.86e-02(3.36e-05)=	<b>6.47e-01(3.42e-06)</b>	6.41e-01(1.57e-05)=
DCF9	1,20	2.50e-02(3.33e-07)	<b>2.46e-02(2.29e-07)=</b>	3.69e-01(4.41e-07)	<b>3.70e-01(1.04e-06)=</b>
	10,20	<b>2.44e-02(2.67e-07)</b>	2.46e-02(1.14e-07)=	<b>3.82e-01(3.79e-07)</b>	3.81e-01(7.60e-07)=
	10,10	<b>2.43e-02(3.47e-07)</b>	2.54e-02(1.45e-07)+	<b>3.82e-01(4.93e-07)</b>	3.80e-01(3.11e-07)+
DCF10	1,20	6.50e-01(2.02e-03)	<b>6.46e-01(1.90e-03)=</b>	1.49e+00(1.25e-02)	1.48e+00(7.30e-03)=
	10,20	<b>6.42e-01(1.12e-03)</b>	6.96e-01(5.37e-04)=	<b>1.48e+00(3.67e-03)</b>	1.36e+00(6.22e-03)=
	10,10	<b>6.56e-01(3.85e-03)</b>	7.14e-01(1.95e-03)=	<b>1.50e+00(1.27e-02)</b>	1.26e+00(4.06e-03)=
DCF11	1,20	<b>3.21e-01(2.51e-04)</b>	3.33e-01(6.97e-05)=	<b>8.56e-01(5.60e-04)</b>	8.51e-01(5.99e-05)=
	10,20	<b>2.45e-01(6.65e-04)</b>	2.49e-01(1.93e-04)=	<b>9.82e-01(1.85e-03)</b>	9.70e-01(1.12e-04)=
	10,10	<b>3.31e-01(8.18e-04)</b>	3.54e-01(1.45e-04)=	<b>8.42e-01(1.62e-03)</b>	8.34e-01(8.97e-05)=
DCF12	1,20	7.71e-01(2.70e-04)	<b>7.58e-01(9.30e-05)=</b>	<b>2.32e-01(1.22e-03)</b>	2.27e-01(1.61e-04)=
	10,20	<b>5.90e-01(1.31e-03)</b>	5.96e-01(5.66e-06)=	<b>5.03e-01(4.75e-03)</b>	5.00e-01(3.66e-06)=
	10,10	5.99e-01(2.44e-03)	<b>5.84e-01(7.27e-05)=</b>	<b>4.92e-01(8.89e-03)</b>	4.91e-01(1.31e-04)=
DCF13	1,20	4.11e-01(2.47e-04)	<b>3.91e-01(3.25e-04)=</b>	6.07e-01(5.28e-04)	<b>6.10e-01(3.45e-04)=</b>
	10,20	4.41e-01(8.01e-04)	<b>4.09e-01(3.82e-04)=</b>	5.67e-01(1.59e-03)	<b>5.78e-01(5.62e-04)=</b>
	10,10	4.53e-01(1.63e-04)	<b>3.82e-01(6.55e-05)=</b>	5.46e-01(3.65e-04)	<b>5.95e-01(2.55e-04)=</b>
DCF14	1,20	<b>1.65e-01(5.64e-05)</b>	2.25e-01(3.43e-04)+	<b>1.17e+00(1.68e-04)</b>	1.05e+00(1.01e-03)+
	10,20	<b>1.88e-01(5.18e-05)</b>	1.97e-01(4.84e-04)=	<b>1.16e+00(1.73e-04)</b>	1.11e+00(7.8e-03)=
	10,10	<b>1.97e-01(7.94e-05)</b>	2.20e-01(1.23e-04)+	<b>1.14e+00(3.36e-04)</b>	1.05e+00(4.58e-04)+

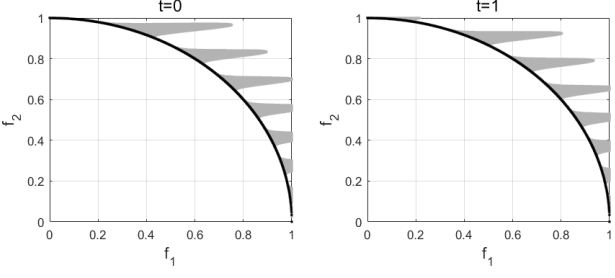


Fig. S-3. DCF1: The overlapped DCPOF and DUPOF are shown in black. The gray area is the feasible region.

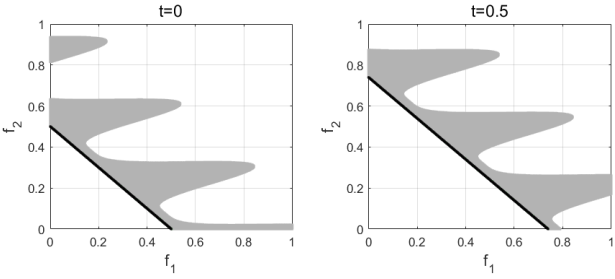


Fig. S-4. DCF2: The overlapped DCPOF and DUPOF are shown in black. The gray area is the feasible region.

#### DCF5:

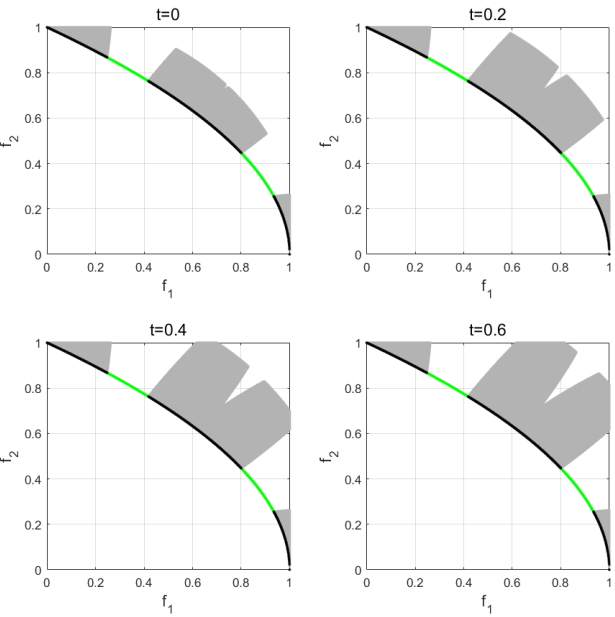


Fig. S-5. DCF3: The DCPOF and DUPOF are shown in black and green, respectively. The gray area is the feasible region.

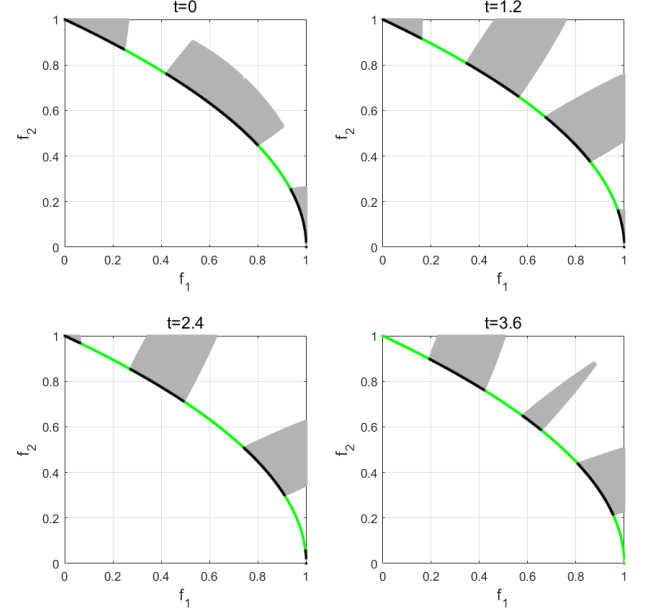


Fig. S-6. DCF4: The DCPOF and DUPOF are shown in black and green, respectively. The gray area is the feasible region.

$$\begin{aligned}
 & \min \begin{cases} f_1(x) = x_1 \\ f_2(x) = g\sqrt{0.5 + G - f_1} \end{cases} \\
 & \text{s.t. } \begin{cases} c_1(x) = 1.1 + C - f_1^2 - f_2^2 \leq 0 \\ c_2(x) = (1 + 0.6 \sin(t + 6l))^2 - f_1^2 - f_2^2 \leq 0 \end{cases} \\
 & G(t) = 0.5|\sin(t)| \\
 & g = 1 + 0.1\left(\left|\sum_{i=2}^D x_i - G\right|\right)^{0.5} \\
 & C(t) = 0.5|\sin(t)| \\
 & l = 0.5\pi - 2|\arctan \frac{f_2}{f_1} - 0.25\pi|
 \end{aligned} \tag{5}$$

The changing DCPOF of DCF5 is always a part of the changing DUPOF. The multiple constraints make the changing feasible region disconnected. Similar to DCF4, the number of disconnected feasible regions changes over time, as shown in Fig. S-7. DCF5 has a changing search space  $[0, 0.5 + G]^D$ .

#### DCF6:

$$\begin{aligned}
 & \min \begin{cases} f_1(x) = x_1 \\ f_2(x) = \begin{cases} g(1 - f_1 - 0.08\sin(5\pi f_1)) & f_1 \geq 0.5 \\ g(G - kf_1 - 0.08\sin(5\pi f_1)) & f_1 < 0.5 \end{cases} \end{cases} \\
 & \text{s.t. } \begin{cases} c_1(x) = C - kf_1 - f_2 - l \leq 0 \\ c_2(x) = 1 - f_1 - f_2 - l \leq 0 \end{cases} \\
 & G(t) = 0.6 + 0.3|\sin(t)| \\
 & g = 1 + 0.1\left(\left|\sum_{i=2}^D x_i - G\right|\right)^{0.5} \\
 & k = 2G - 1 \\
 & C(t) = 0.6 + 0.3|\sin(t)| \\
 & l = 0.08\sin(5\pi f_1))
 \end{aligned} \tag{6}$$

The DUPOF of DCF6 is partially changed, and the DCPOF remains the same location and is a part of the changing DUPOF. The feasible region of DCF6 can become very narrow, as shown in Fig. S-8. DCF6 has a changing search space  $[0, 0.5 + G]^D$ .

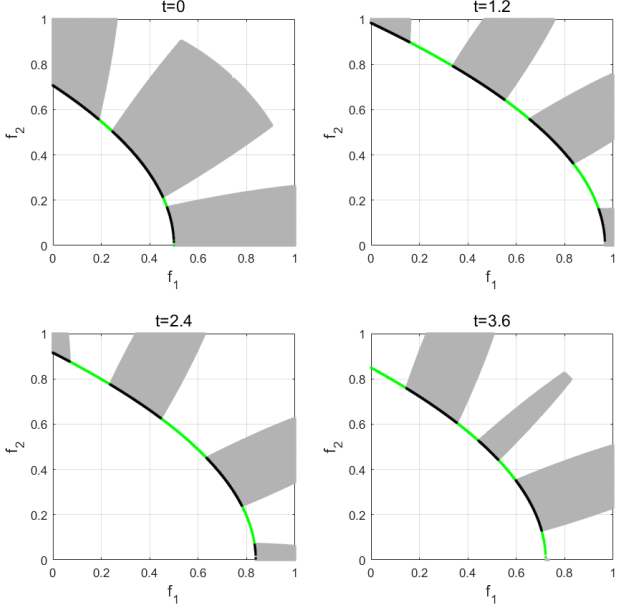


Fig. S-7. DCF5: The DCPOF and DUPOF are shown in black and green, respectively. The gray area is the feasible region.

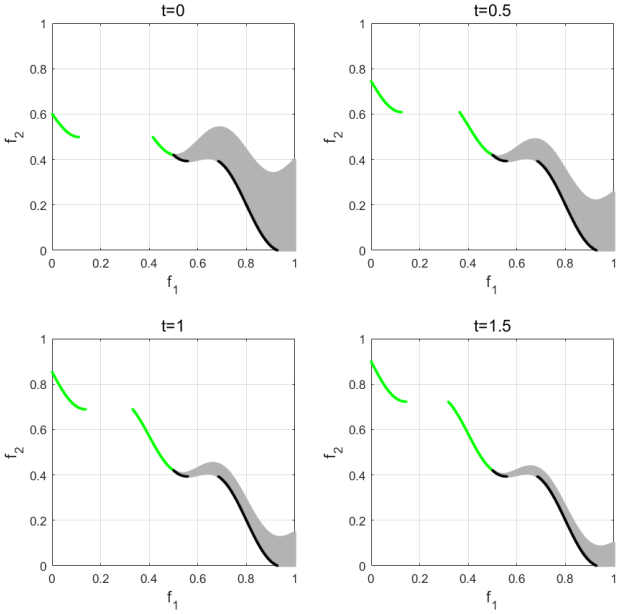


Fig. S-8. DCF6: The DCPOF and DUPOF are shown in black and green, respectively. The gray area is the feasible region.

#### DCF7:

$$\begin{aligned} & \min \left\{ \begin{array}{l} f_1(x) = x_1 \\ f_2(x) = g\sqrt{1 - f_1^2} \end{array} \right. \\ & \text{s.t. } \left\{ \begin{array}{l} c_1(x) = 1.1 - f_1^2 - f_2^2 + 0.125\sin(0.1 + 2\pi l)^4 \geq 0 \\ c_2(x) = 1 - f_1^2 - f_2^2 + 0.125\sin(0.1 + 2\pi l)^4 \leq 0 \end{array} \right. \\ & G(t) = |\sin(t)| \\ & g = 1 + 0.1(|\sum_{i=2}^D x_i - G|)^{0.5} \\ & l = \sqrt{2}f_2 - \sqrt{2}f_1 \end{aligned} \quad (7)$$

The DCPOF of DCF7 consists of a part of the DUPOF and

a part of the boundary of the feasible region, as shown in Fig. S-9. DCF7 belongs to Type I DCMOP, that is, the DCPOF and DUPOF are unchanged. Moreover, DCF7 has a narrow connected feasible region. The search space is  $[0, 1]^D$ .

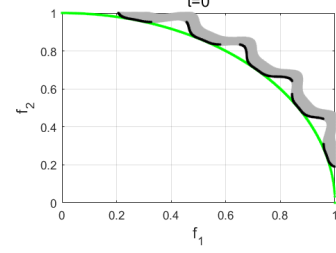


Fig. S-9. DCF7: The DCPOF and DUPOF are shown in black and green, respectively. The gray area is the feasible region.

#### DCF8:

$$\begin{aligned} & \min \left\{ \begin{array}{l} f_1(x) = x_1 \\ f_2(x) = g(1 - f_1) \end{array} \right. \\ & \text{s.t. } \left\{ \begin{array}{l} c_1(x) = f_1 + f_2 - 1.4 - \frac{\sin(t)\sin(t+l)^6}{2} \leq 0 \\ c_2(x) = 0.95 - f_1 - f_2 + 0.235\sin(t + l)^2 \leq 0 \end{array} \right. \\ & G(t) = |\sin(t)| \\ & g = 1 + 0.1(|\sum_{i=2}^D x_i - G|)^{0.5} \\ & l = 0.75\pi(\sqrt{2}f_2 - \sqrt{2}f_1) \end{aligned} \quad (8)$$

The DCPOF of DCF8 consists of a part of the DUPOF and a part of the boundary of the feasible region. In addition, The connectivity of the feasible region changes over time, and DCF8 contains a narrow feasible region, as shown in Fig. S-10. The search space is  $[0, 1]^D$ .

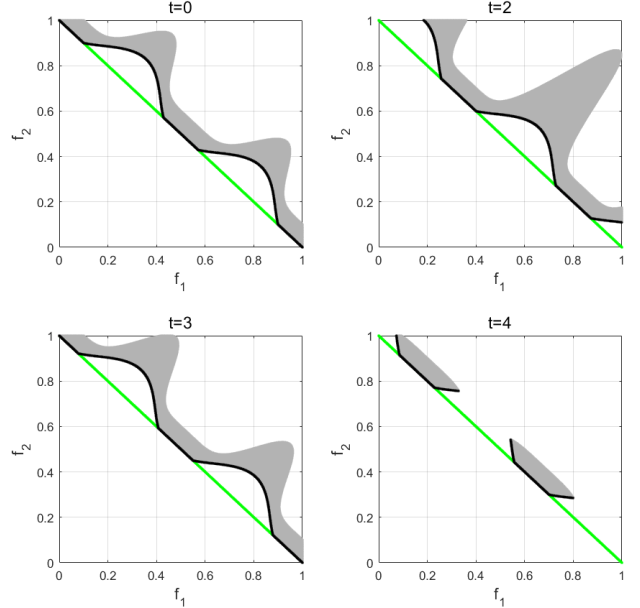


Fig. S-10. DCF8: The DCPOF and DUPOF are shown in black and green, respectively. The gray area is the feasible region.

#### DCF9:

$$\begin{aligned}
& \min \left\{ \begin{array}{l} f_1(x) = x_1 \\ f_2(x) = g\sqrt{0.5 + G - f_1} \end{array} \right. \\
& \text{s.t. } \left\{ \begin{array}{l} c_1(x) = G + 0.7 - f_1 - f_2^2 + 0.3\sin(10\pi l_1) \leq 0 \\ c_2(x) = G + 0.5 - f_1 - f_2^2 + 0.11\sin(t + 2\pi l_2) \leq 0 \end{array} \right. \\
& G(t) = 0.5|\sin(t)| \\
& g = 1 + 0.1(|\sum_{i=2}^D x_i - G|)^{0.5} \\
& l_1 = \arctan \frac{f_2}{f_1} \\
& l_2 = \sqrt{2}f_2 - \sqrt{2}f_1
\end{aligned} \tag{9}$$

The DCPOF of DCF9 consists of a part of the DUPOF and a part of the boundary of the feasible region. DCF9 is a Type IV DCMOP, the DUPOF and DCPOF are changing over time, as shown in Fig. S-11. The changing search space is  $[0, 0.5 + G]^D$ .

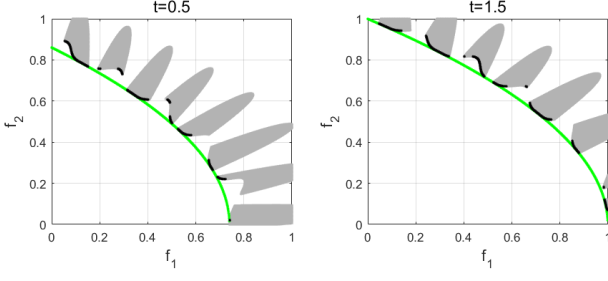


Fig. S-11. DCF9: The DCPOF and DUPOF are shown in black and green, respectively. The gray area is the feasible region.

DCF10:

$$\begin{aligned}
& \min \left\{ \begin{array}{l} f_1(x) = x_1 \\ f_2(x) = g(G + kf_1) \end{array} \right. \\
& \text{s.t. } \left\{ \begin{array}{l} c_1(x) = -(3 - 0.7f_1^2 - f_2)^{l_1} \leq 0 \\ c_2(x) = (3 - 0.325f_1^2 - f_2)^{l_2} \leq 0 \\ c_3(x) = -(1.42 + 0.11f_1^2 - f_2)^{l_3} \leq 0 \\ c_4(x) = (2.07 - 0.03f_1^2 - f_2)^{l_4} \leq 0 \end{array} \right. \\
& G(t) = 1.712565 + 0.138755 \sin(t) \\
& k = 1 - G \\
& g = 1 + 0.1(|\sum_{i=2}^D x_i - G|)^{0.5} \\
& l_1 = 3 - 2f_1^2 - f_2 \\
& l_2 = 3 - 7f_1^2 - f_2 \\
& l_3 = 1.025 - 0.025f_1^2 - f_2 \\
& l_4 = 0.3 + 0.05f_1^2 - f_2
\end{aligned} \tag{10}$$

The DCPOF of DCF10 consists of an isolated point ( $f_1 = 1, f_2 = 1$ ) located on the DUPOF and a part of the boundary of the feasible region. The distance between DUPOF and DCPOF changes over time, as shown in Fig. S-12. DCF10 has four constraints and these constraints make the gap between different disconnected feasible regions huge. The changing search space is  $[0, 0. - G/k]^D$ .

DCF11:

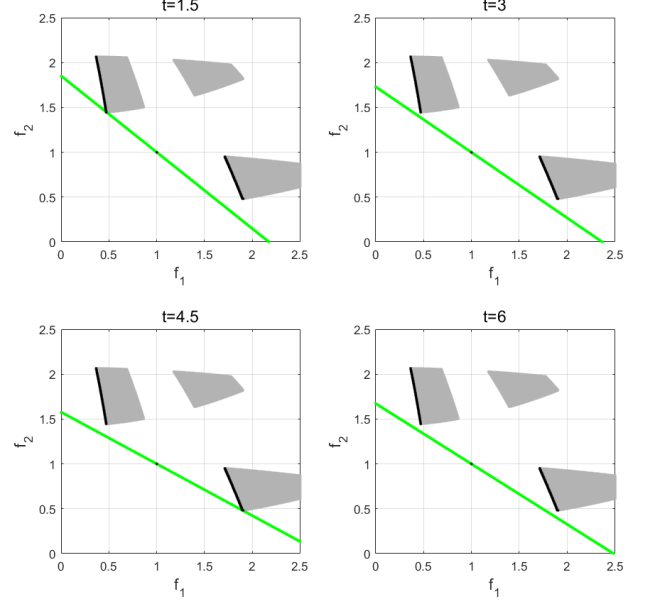


Fig. S-12. DCF10: The DCPOF and DUPOF are shown in black and green, respectively. The gray area is the feasible region.

$$\begin{aligned}
& \min \left\{ \begin{array}{l} f_1(x) = x_1 \\ f_2(x) = g(0.95 - 0.8f_1 - 0.08|\sin(3.2\pi f_1)|) \end{array} \right. \\
& \text{s.t. } \left\{ \begin{array}{l} c_1(x) = (1 - 0.8f_1 - f_2 + l_1)^{1.8 - 1.125f_1 - f_2 + l_2} \leq 0 \\ c_2(x) = (1 - 0.625f_1 - f_2 + l_3)^{1.4 - 0.875f_1 - f_2 + l_4} \geq 0 \end{array} \right. \\
& G(t) = |\sin(t)| \\
& g = 1 + 0.1(|\sum_{i=2}^D x_i - G|)^{0.5} \\
& l_1 = 0.08 \sin(2\pi(f_2 - f_1/1.5)) \\
& l_2 = 0.08 \sin(2\pi(f_2/1.8 - f_1/1.6)) \\
& l_3 = 0.08 \sin(2\pi(f_2 - f_1/1.6)) \\
& l_4 = 0.08 \sin(2\pi(f_2/1.4 - f_1/1.6))
\end{aligned} \tag{11}$$

The objective space of DCF11 is given in Fig. S-13. DCF11 is derived from MW12 [1] and belongs to Type I DCMOP. The DUPOF of DCF11 is entirely located outside the feasible region. Thus, the DCPOF is composed of a part of the boundary of the feasible region. DCF11 has a disconnected feasible region. The search space of DCF11 is  $[0, 1]^D$ .

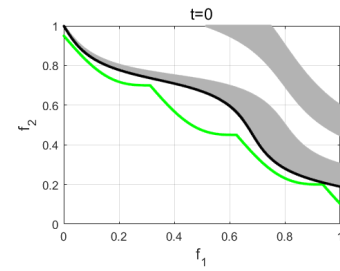


Fig. S-13. DCF11: The DCPOF and DUPOF are shown in black and green, respectively. The gray area is the feasible region.

DCF12:

$$\begin{aligned}
& \min \left\{ \begin{array}{l} f_1(x) = x_1 \\ f_2(x) = g(0.95 - 0.8f_1 - 0.08|\sin(3.2\pi f_1)|) \end{array} \right. \\
& \text{s.t. } \left\{ \begin{array}{l} c_1(x) = (1 - 0.8f_1 - f_2 + l_1)^{1.8 - 1.125f_1 - f_2 + l_2} \leq 0 \\ c_2(x) = \begin{cases} (l_3)^{l_4} \geq 0 & \text{if } \sin(5\pi t) = 0 \\ (l_3)^{l_4} < 0 & \text{otherwise} \end{cases} \\ G(t) = |\sin(t)| \\ g = 1 + 0.1(\sum_{i=2}^D x_i - G|)^{0.5} \\ l_1 = 0.08 \sin(2\pi(f_2 - f_1/1.5)) \\ l_2 = 0.08 \sin(2\pi(f_2/1.8 - f_1/1.6)) \\ l_3 = 1 - 0.625f_1 - f_2 + 0.08 \sin(2\pi(f_2 - f_1/1.6)) \\ l_4 = 1.4 - 0.875f_1 - f_2 + 0.08 \sin(2\pi(f_2/1.4 - f_1/1.6)) \end{array} \right. \\
& \quad (12)
\end{aligned}$$

DCF12 is derived from DCF11 and belongs to Type II DCMOP. The connectivity of DCF12 changes over time. To be specific, the connectivity is from connected to disconnected to connected, as shown in Fig. S-14. In particular, the feasible regions of two consecutive time steps are non-overlapping and complementary, i.e., the feasible region at  $t = 0$  changes to an infeasible region at  $t = 1$ . The search space of DCF12 is  $[0, 1]^D$ .

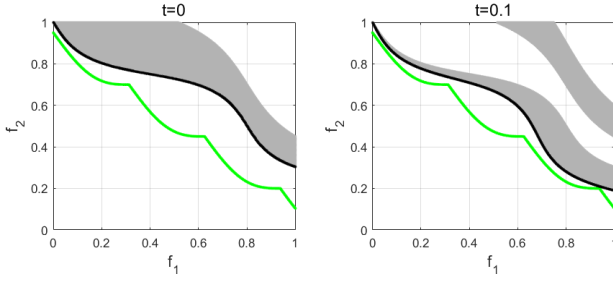


Fig. S-14. DCF12: The DCPOF and DUPOF are shown in black and green, respectively. The gray area is the feasible region.

DCF13:

$$\begin{aligned}
& \min \left\{ \begin{array}{l} f_1(x) = x_1 \\ f_2(x) = g(G - 0.8f_1 - 0.08|\sin(3.2\pi f_1)|) \end{array} \right. \\
& \text{s.t. } \left\{ \begin{array}{l} c_1(x) = (1 - 0.8f_1 - f_2 + l_1)^{2G - 1.125f_1 - f_2 + l_2} \leq 0 \\ c_2(x) = (G + 0.15 - 0.625f_1 - f_2 + l_3)^{l_4} \geq 0 \\ G(t) = 0.85 + 0.05 \sin(t) \\ g = 1 + 0.1(\sum_{i=2}^D x_i - G|)^{0.5} \\ l_1 = 0.08 \sin(2\pi(f_2 - f_1/1.5)) \\ l_2 = 0.08 \sin(2\pi(f_2/1.8 - f_1/1.6)) \\ l_3 = 0.08 \sin(2\pi(f_2 - f_1/1.6)) \\ l_4 = 1.4 - 0.875f_1 - f_2 + 0.08 \sin(2\pi(f_2/1.4 - f_1/1.6)) \end{array} \right. \\
& \quad (13)
\end{aligned}$$

DCF13 is also derived from DCF11 and belongs to Type IV DCMOP, i.e., the DUPOF and DCPOF are both changing over time and the DUPOF is always outside of the feasible region. As shown in Fig. S-15, the size of two unconnected feasible regions will change over time. The search space of DCF13 is  $[0, 1]^D$ .

DCF14:

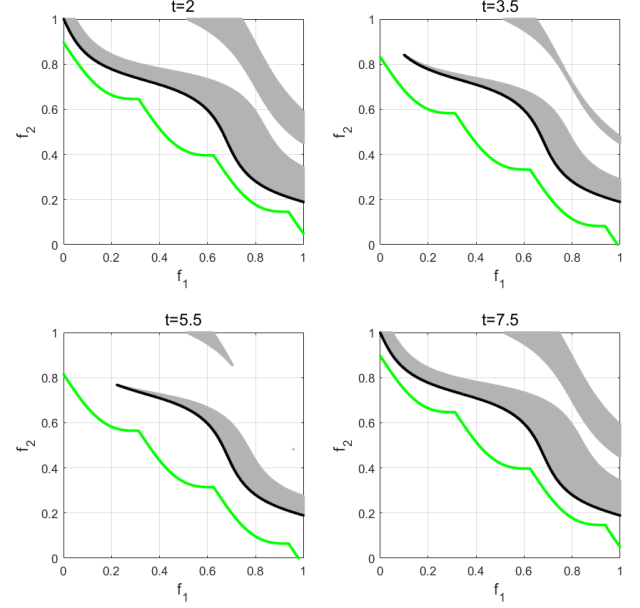


Fig. S-15. DCF13: The DCPOF and DUPOF are shown in black and green, respectively. The gray area is the feasible region.

$$\begin{aligned}
& \min \left\{ \begin{array}{l} f_1(x) = x_1 \\ f_2(x) = g(0.8 - 0.8f_1 - 0.1 \sin(3.2\pi f_1(t \bmod 4))) \end{array} \right. \\
& \text{s.t. } \left\{ \begin{array}{l} c_1(x) = (1 - 0.8f_1 - f_2 + l_1)^{1.8 - 1.125f_1 - f_2 + l_2} \leq 0 \\ c_2(x) = (1 - 0.625f_1 - f_2 + l_3)^{1.4 - 0.875f_1 - f_2 + l_4} \geq 0 \\ G(t) = 0.85 + 0.05 \sin(t) \\ g = 1 + 0.1(\sum_{i=2}^D x_i - G|)^{0.5} \\ l_1 = 0.08 \sin(2\pi(f_2 - f_1/1.5)) \\ l_2 = 0.08 \sin(2\pi(f_2/1.8 - f_1/1.6)) \\ l_3 = 0.08 \sin(2\pi(f_2 - f_1/1.6)) \\ l_4 = 0.08 \sin(2\pi(f_2/1.4 - f_1/1.6)) \end{array} \right. \\
& \quad (14)
\end{aligned}$$

Similarly, DCF14 is derived from DCF11 and belongs to Type III DCMOP. The DUPOF will change from a linear geometry to a disconnected geometry over time, as shown in Fig. S-16. The search space of DCF14 is  $[0, 1]^D$ .

## REFERENCES

- [1] Z. Ma and Y. Wang, "Evolutionary constrained multiobjective optimization: Test suite construction and performance comparisons," *IEEE Transactions on Evolutionary Computation*, vol. 23, no. 6, pp. 972–986, 2019.

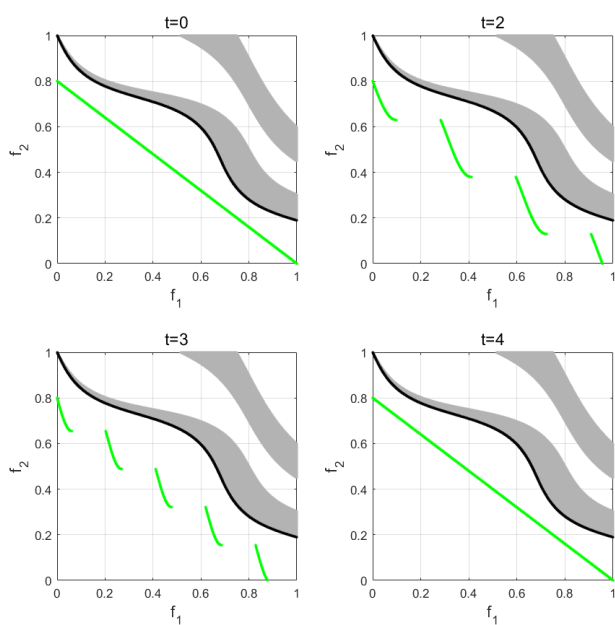


Fig. S-16. DCF14: The DCPOF and DUPOF are shown in black and green, respectively. The gray area is the feasible region.